Thermal Diffusivities of Continuous Casting Powders for Steel at High Temperature

Y. Waseda, M. Masuda, K. Watanabe, H. Shibata
Institute for Advanced Materials Processing, Tohoku University, Sendai 980, Japan

H. Ohta
Department of Materials Science, Ibaraki University, Hitachi 316, Japan

K. Nakajima
R & D Center, Sumitomo Metal Industry Co. Ltd., Amagasaki 660, Japan

(Received January 21, 1994; final form March 25, 1994)

ABSTRACT

Thermal diffusivity measurements of continuous casting powders for steel have systematically been carried out at high temperature by the laser flash method. The powder samples consist of SiO_2, Al_2O_3, MgO, CaO, Na_2O and CaF_2 with the addition of TiO_2, ZrO_2, HfO_2 or iron oxide. At higher temperature, the measured values obtained by the laser flash method are known to involve, more or less, the contribution due to radiative component. Therefore, the thermal diffusivities of continuous casting powders for steel were estimated with sufficient reliability by separating such radiative component from measured values after due consideration for the variation of their absorption coefficients. The correction for radiative component is significant in samples including TiO_2, ZrO_2 or iron oxide, because these samples show the significant variation in the absorption coefficients.

1. INTRODUCTION

Heat transfer properties such as the thermal diffusivity of high temperature melts with sufficient reliability are essential in order to design various manufacturing plants. This includes continuous casting powder melts consisting of SiO_2-Al_2O_3-MgO-CaO-Na_2O-CaF_2 for further improving the present continuous casting process for steel /1/. However, thermal diffusivity measurements of high temperature melts are still far from complete in various cases, arising mainly from onset convective heat flow, heat leak to the container and mixed contributions of radiative and conductive heat transfer components. Thus, the available thermal diffusivity data with sufficient reliability at high temperature are limited to only a small number of compositions.

The laser flash method has recently been recognized as one of the most versatile techniques for measuring thermal diffusivity of various materials. Particularly, a three layered cell by the laser flash method on the differential scheme has been successfully developed for determining the thermal diffusivity of high temperature melts /2,3/.

The main purpose of this work is to describe the thermal diffusivity values of continuous casting powders for steel with various compositions systematically determined by applying the differential

three layered laser flash method and by precisely separating the radiative component from measured values after due consideration for the variation of the absorption coefficients of powder samples.

2. EXPERIMENTAL PROCEDURES AND THEORETICAL BASIS

Figure 1 shows the schematic diagram for the laser flash apparatus including a three layered cell system for measuring the thermal diffusivity of a liquid sample at high temperatures. A platinum crucible containing a small amount of a liquid sample is placed on the alumina pipe. The size of this crucible (corresponding to the third layer) is 0.2 mm thick, 10 mm deep and 19 mm in diameter. Another relatively small platinum crucible of 0.2 mm thickness, 14 mm depth and 14 mm diameter is employed as the first layer and it is centered to the end of an alumina tube by ceramic cement (Aron ceramic-D, Touwa-gousei Chem. Industry, Japan). The alumina tube is connected to a holder on a three axial

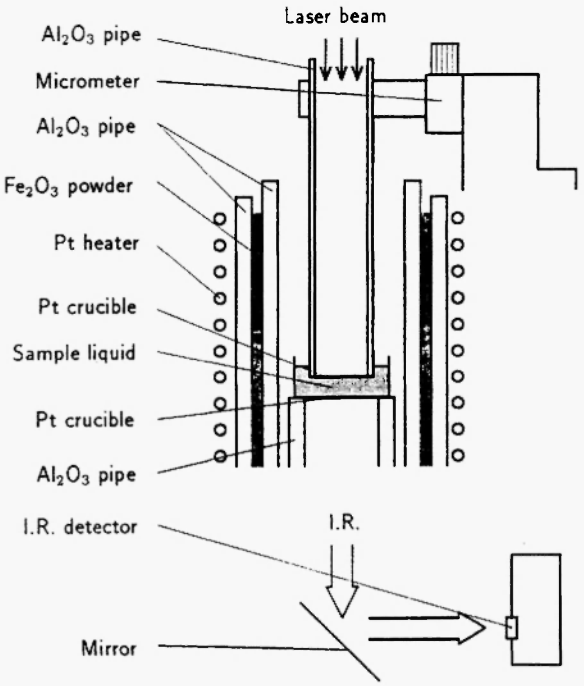

Fig. 1: The schematic diagram of the three layered laser flash apparatus for measuring thermal diffusivity of a liquid sample at high temperature.

movable arm and the upper platinum crucible is located just right above the lower one to make a three layered cell system. The cell system itself was heated in a platinum wounded furnace under the air atmosphere.

The inner and outer platinum crucibles were separated several times during the course of the experiments to check that there was no bubble in a liquid sample. The tube was lowered vertically by loosening the holder screw at the desired thickness, and fixed. Then a pulsed ruby laser beam was flashed on the top surface of the inner crucible (the first layer). The temperature response curve was obtained by means of an InSb infra-red detector focused on the back surface of the outer crucible (the third layer) through a gold mirror. Another temperature response curve was measured after changing the thickness of a liquid sample. The variation of the sample thickness can be determined by reading a micrometer scale attached on the holder. In this work, the difference of sample thickness $\Delta\tau$ in two sets of the measurements was fixed to be 0.2 mm, on the basis of the previous results on high temperature melts using the three-layered laser flash method /2,3/.

An easy and reliable data processing method has been developed to estimate the thermal diffusivity of a liquid sample at high temperature using the three layered laser flash method /3/. Only the essential points are given below for convenience of discussion.

The temperature response of a three layered cell at the initial time region of the temperature response curve may be expressed in the following form, analogous to the approach for a two layered cell proposed by James /4/.

$$\frac{\partial \ln(\theta\sqrt{t})}{\partial(1/t)} = -\frac{(\eta_1 + \eta_2 + \eta_3)^2}{4} \qquad (1)$$

where η_i is $l_i\sqrt{\alpha_i}$. Thus, a plot of $\ln(\theta\sqrt{t})$ against 1/t for eq. (1) gives a straight line with slope of $-(\eta_1 + \eta_2 + \eta_3)^2/4$. The thermal diffusivity value of α_2 of the second layer (a liquid sample in the present case) can readily be determined, when the thermal diffusivity values of the first and third layers and the thickness of all three layers are known.

Let us consider an infinite slab as shown in Fig. 2 consisting of three layers. The thickness and thermal

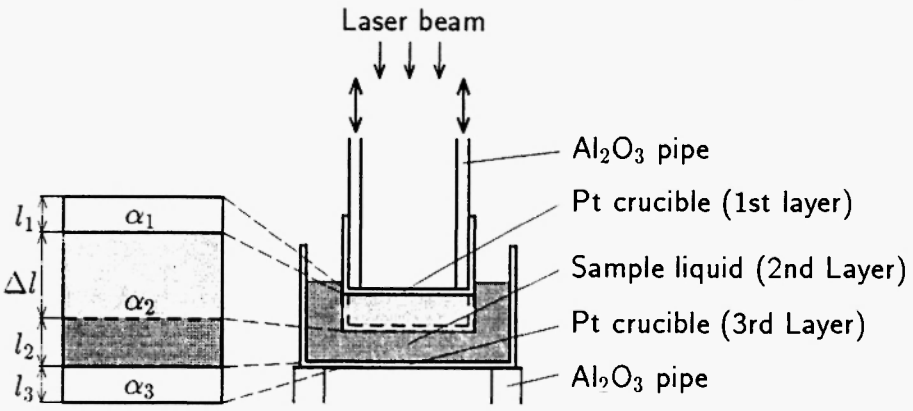

Fig. 2: The schematic diagram of the cell assembly employed in this work with differential scheme.

diffusivity of the i-th layer are denoted by l_i and α_i, respectively. The upper plate is designated as the first layer. Similarly, a liquid sample and the bottom plate are considered as the second and third layers. At the initial time region, the temperature response of the back surface of the third layer can be described as eq. (1). Then, the following equation may be obtained:

$$l_2/\sqrt{\alpha_2} = 2\sqrt{-\frac{\partial \ln(\theta_{(l_2)}\sqrt{t})}{\partial(1/t)}} - \eta_1 - \eta_3 \qquad (2)$$

$$(l_2 + \Delta l)/\sqrt{\alpha_2} = 2\sqrt{-\frac{\partial \ln(\theta_{(l_2+\Delta l)}\sqrt{t})}{\partial(1/t)}} - \eta_1 - \eta_3 \qquad (3)$$

l_2 is the thickness of a liquid sample in the first measurement and Δl is the relative change of thickness of a liquid sample corresponding to the difference of sample thickness between two measurements produced by lifting up the upper plate (the first layer in the present case). The relation between the sample thickness l_2 and the sample thermal diffusivity α_2 is given as a solid line in Fig. 3. For a given Δl, the similar relation between l_2 and $l_2 + \Delta l$ is also obtained as a dashed line in Fig. 3. The intersection of these two lines provides the resultant thermal diffusivity value of a liquid sample α_2 and its thickness l_2. More detailed information for this data processing is given in ref. /3/. It may also be noted from the recent results by the finite element method of computer simulation that the heat leak through a side wall of a platinum crucible using the three layered laser flash method is able to reduce less than 5%, when only the values of sample thickness and its variation are carefully selected /5/.

3. RESULTS AND DISCUSSION

Table 1 gives the chemical composition of 19 synthetic continuous casting powder samples for steel presently investigated. The measured thermal diffusivity values are shown in Fig. 4 using the results of samples containing TiO_2 and iron oxide as an example. Although there are differences in detail, similar results were obtained for all other cases. The results of Fig. 4 indicate a slight positive temperature coefficient of thermal diffusivity of these powder samples in the temperature range presently measured. However, it should be mentioned that the present results are somewhat spread in certain temperatures. Such scattering exceeds the experimental uncertainty and it is attributed to the effect of radiative heat transfer component in a liquid sample. The radiative component should be separated from measured value, although the initial time region of the temperature response curve is known not to be severely affected by the radiative heat transfer /4/. This is particularly true at higher temperatures.

Quantitative discussion of the radiative heat transfer in high temperature substances requires the optical properties such as the absorption coefficient of samples in question. Such information is essential for the semi-transparent media, compared with the transparent and opaque cases. Figure 5 gives the absorption coefficients of three samples as a function of wave length together with that of the hemispherical emissive power of blackbody at 1573 K /6/. It should be mentioned that the change in CaO/SiO_2 ratio or the addition of ZrO_2

Table 1

Chemical composition of synthetic continuous casting powders for steel in mass %.

Type of slag		SiO_2	CaO	CaF_2	Na_2O	MgO	Al_2O_3	ZrO_2	HfO_2	TiO_2	Fe
Reference		35.6	19.9	17.1	10.1	9.3	7.7	(CaO/SiO_2	0.902)		
ZrO_2	0.8%	36.0	21.0	15.8	10.0	9.4	7.5	0.8			
ZrO_2	2.5%	36.0	21.9	13.8	9.4	9.1	7.4	2.5			
ZrO_2	4.9%	35.0	20.3	15.2	9.6	8.8	7.2	4.9			
ZrO_2	7.6%	33.7	20.5	14.0	9.5	8.7	6.9	7.6			
ZrO_2	10.0%	32.8	19.1	14.2	9.1	8.7	6.9	10.0			
HfO_2	0.7%	35.0	19.4	18.3	10.3	9.0	7.3		0.7		
HfO_2	5.1%	33.4	18.5	17.5	9.9	8.6	7.0		5.1		
HfO_2	9.8%	31.7	17.6	16.6	9.4	8.2	6.7		9.8		
TiO_2	0.7%	36.3	21.1	16.4	9.8	7.9	7.5			0.7	
TiO_2	2.6%	34.8	21.2	16.0	9.2	9.1	7.2			2.6	
TiO_2	4.9%	33.9	21.6	15.0	8.5	8.8	7.7			4.9	
TiO_2	7.4%	33.0	20.8	14.6	8.7	8.6	7.6			7.4	
TiO_2	9.6%	32.5	19.6	15.0	8.7	8.5	7.5			9.6	
Fe	0.4%	36.1	21.0	15.6	9.3	8.9	8.4				0.4
Fe	1.2%	35.7	21.7	15.0	9.1	8.7	8.3				1.2
Fe	2.6%	34.9	20.9	15.0	9.3	8.7	8.1				2.6
CaO/SiO_2	0.637	42.1	15.7	15.4	9.4	9.1	8.3				
CaO/SiO_2	1.245	30.6	26.3	16.4	9.4	9.5	8.5				

and HfO_2 to the reference composition appears not to vary significantly the absorption coefficient in the range between 1 x 10^{-6} and 4 x 10^{-6} m^{-1} /6/ and the correction by the transparent body approximation is well accepted for these samples with respect to the radiative heat transfer behavior. In other words, the contribution due to radiative component should be explicitly considered only for samples containing TiO_2 and iron oxide.

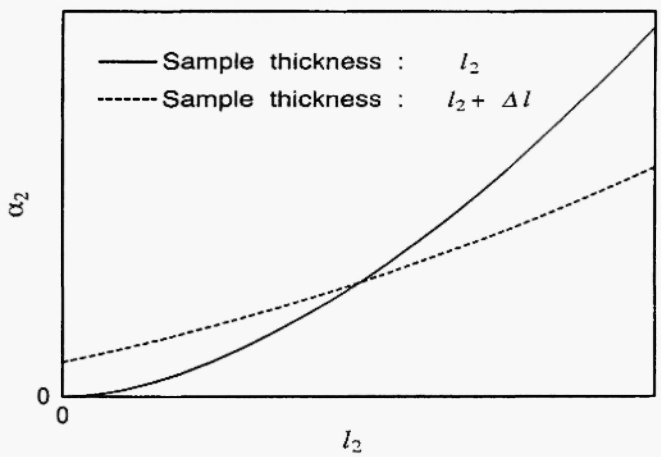

Fig. 3: Thermal diffusivity of α_2 as a function of sample thickness of l_2 from the relations of eqs. (2) and (3).

In the transparent body approximation, a liquid layer is considered to be transparent to radiative heat transfer where no radiation is absorbed or emitted from a liquid layer, and the radiation from a platinum plate is dominant. Ohta *et al.* /7/ have systematically investigated the effect of radiative component in the transparent body approximation by estimating the apparent thermal diffusivity values for a sample of thermal diffusivity of $\alpha_0 = 4 \times 10^{-7}$ m^2/s using the finite difference method in numerical computation. For convenience, an essential point is given in Fig. 6 indicating that the apparent thermal diffusivity values increase with increasing temperature and sample thickness by the contribution due to radiative component. These results also suggest that the radiative component provides an increase of about 20% in thermal diffusivity for the measurement where the sample thickness of 0.1 mm (for the first measurement) with its variation of 0.2 mm. The coefficients are

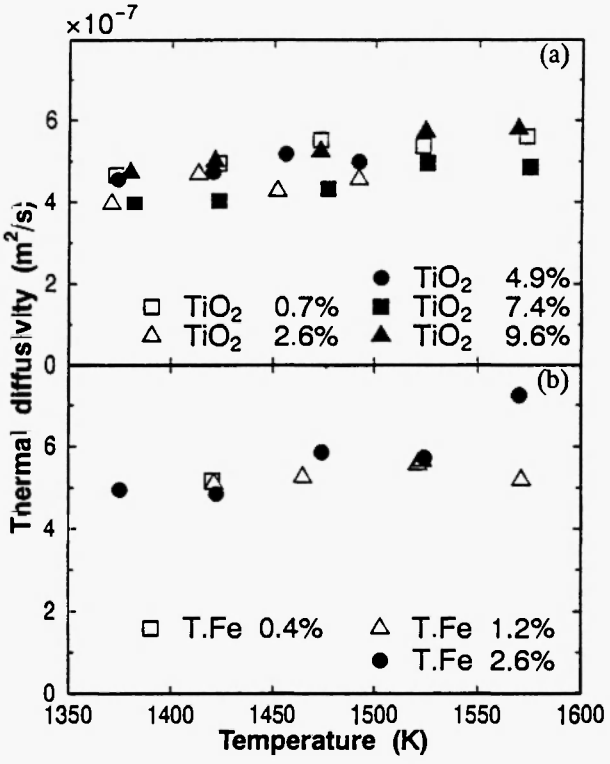

Fig. 4: Thermal diffusivity values of samples containing TiO_2 and iron oxide. These values, more or less, include the contribution due to radiative component at high temperature.

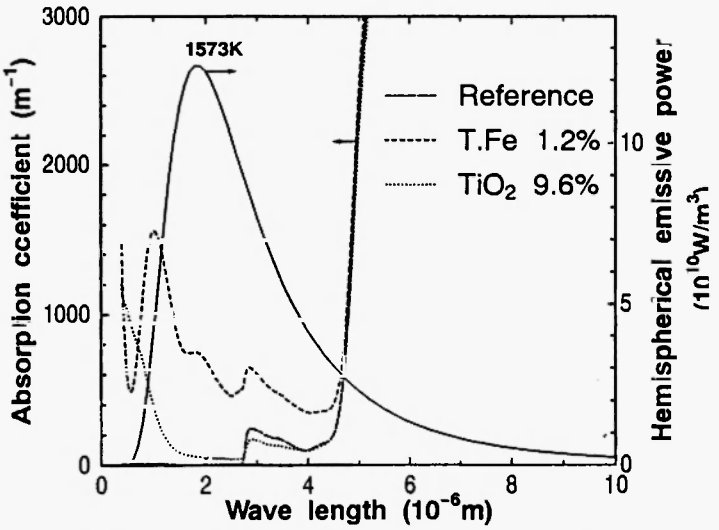

Fig. 5: Absorption coefficient of powders containing TiO_2 and iron oxide together with the hemispherical spectral emissive power of blackbody at 1573 K /6/.

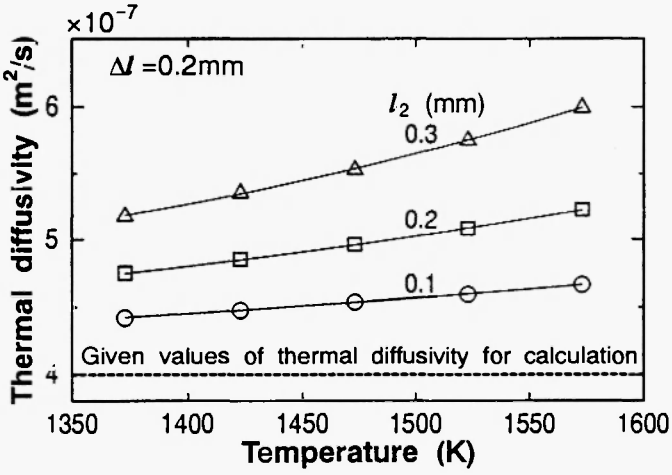

Fig. 6: Apparent thermal diffusivity including radiative heat flow theoretically estimated under the transparent body approximation for a sample of thermal diffusivity of 4 x 10^{-7} m^2/s /7/.

summarized in the following as a function of the absolute temperature T.

$$\alpha = c\alpha_o \qquad (4)$$

$$\left.\begin{aligned} c &= 2.549\times10^{-7}T^2 - 4.504\times10^{-4}T + 1.244 \quad \text{for } l_2=0.1 \text{ mm} \\ c &= 6.986\times10^{-7}T^2 - 1.466\times10^{-3}T + 1.883 \quad \text{for } l_2=0.2 \text{ mm} \\ c &= 1.253\times10^{-6}T^2 - 2.675\times10^{-3}T + 2.606 \quad \text{for } l_2=0.3 \text{ mm} \end{aligned}\right\} \qquad (5)$$

Measured thermal diffusivity values should be corrected using these factors with the value of l_2.

When the transparent body approximation is not well accepted as for a sample including iron oxide, the absorption and emission in a liquid layer should be considered. Regarding this subject, Darby /8/ has already proposed fundamental equations by considering all modes of radiative heat transfer, and Ohta *et al.* /7/ also report the results of the gray body approximation where the spectral absorption coefficient of the semi-

transparent media is reduced to the mean absorption coefficient κ_m using Darby's equations coupled with the control volume method /9/. The temperature response is calculated as a function of κ_m and then the thermal diffusivity values can be estimated. The results are shown in Fig. 7 for the sample of thermal diffusivity of 4 x 10^{-7} m^2/s /7/. The validity and usefulness of the present results may be confirmed by suggesting the following points. Good agreement is found with the value proposed by Rosseland /10/, who suggests for the condition of $\kappa l > 1$, in the higher absorption region larger than 10^5 m^{-1}. When the absorption coefficient is over 10^6 m^{-1}, a sample is considered to be opaque and then the radiative contribution is insignificant. On the other hand, in the lower absorption region less than 10^2 m^{-1}, the results are consistent with those of the transparent body approximation. It is also clearly drawn from the results of Fig. 7 that the contribution due to radiative component should be separated from measured thermal diffusivity values using, at least, the gray body approximation or higher order (band) approximation in cases where the absorption coefficient is 10^2 to 10^4 m^{-1}. Samples containing TiO_2 and iron oxide are included in this category. Table 2 shows the mean absorption coefficient κ_m of samples containing TiO_2 and iron oxide determined from the measurements of spectral transmissivity and reflectivity in the wave length region between 4 x 10^{-7} m and 1 x 10^{-5} m /6/.

Recently Ohta *et al.* /11/ made a numerical estimation regarding the contribution of radiative component at high temperature measurements using the three layered laser flash method; they considered the variation of the optical properties of samples and provided information about the apparent thermal diffusivity values theoretically calculated for three cases of the transparent body approximation, the gray body approximation and the band approximation. It may be noted that the wave length dependence of the absorption coefficient, as exemplified by the results of Fig. 5, is explicitly included in the band approximation, although this requires lengthy numerical computation. The theoretical details are given in the Appendix for further convenience. The most important and significant aspects of their results are summarized in Table 3, providing the variation of the apparent thermal

Table 2

Mean absorption coefficient κ_m for samples containing TiO_2 and iron oxide estimated from measured optical properties /6/

Temperature (K)		1373	1473	1573
Type of powder		κ_m		
Fe	0.4%	546	572	596
Fe	1.2%	774	810	844
TiO_2	2.6%	21	22	24
TiO_2	4.9%	39	41	43
TiO_2	9.6%	81	87	94

Table 3

Apparent thermal diffusivity estimated from theoretical temperature response curves at 1575 K by the three layered laser flash method. Given thermal diffusivity: 4 x 10^{-7} m^2/s, sample thickness and its variation: 0.2 mm and 0.2 mm. The numerical values in the parenthesis correspond to the ratio of deviation from the case estimated under the band approximation /11/.

Type of powder		Approximation				
		Transparent		Gray		Band
Reference		4.90	(0.03)			5.05
Fe	0.4%	4.90	(0.09)	5.29	(0.02)	5.39
Fe	1.2%	4.90	(0.11)	5.44	(0.01)	5.50
TiO_2	2.6%	4.90	(0.04)	4.91	(0.04)	5.10
TiO_2	4.9%	4.90	(0.04)	4.93	(0.03)	5.11
TiO_2	9.6%	4.90	(0.05)	4.97	(0.03)	5.13

diffusivity values when using three different approximations for estimating the radiative contribution. The contribution due to radiative component could be estimated by the transparent body approximation with an experimental uncertainty of less than 4% for samples considered transparent. On the other hand, the contribution due to radiative component should be estimated, at least, by the gray body approximation using the mean absorption coefficient for samples recognized as semi-transparent if we want to hold the experimental uncertainty down to less than 4%.

With these facts in mind, the contribution due to radiative component was quantitatively separated from measured thermal diffusivity values of 19 continuous casting powders for steel in this work by applying the

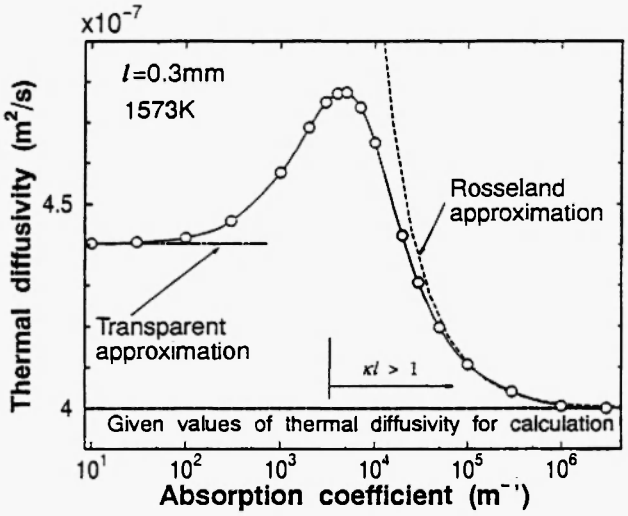

Fig. 7: Apparent thermal diffusivity including radiative heat flow theoretically estimated at 1573 K under the gray body approximation for a sample of thermal diffusivity of 4 x 10^{-7} m^2/s /7/.

transparent body approximation or the gray body approximation, depending upon the absorption coefficient behavior. The resultant thermal diffusivity values are illustrated in Fig. 8 using the results of samples containing TiO_2 and iron oxide. When comparing the results of Fig. 4, it is clearly found that scattering detected in measured values is considerably reduced by correcting the contribution due to radiative component, depending upon both temperature and sample thickness. In addition, the thermal diffusivity values of continuous casting powders for steel are of the order of $4 \pm 0.5 \times 10^{-7}$ m^2/s and insignificant with the variation of temperature and concentration presently investigated. It is also worth mentioning that the thermal diffusivity values obtained in this work can be expressed with sufficient reliability in the form of $\alpha(10^{-7}\ m^2/s) = aT + b$ where T is the absolute temperature and the values of a and b determined by a least squares analysis are given in Figs. 8 and 9. It would be interesting to extend the present results so as to discuss heat transfer behavior in the continuous casting process for steel.

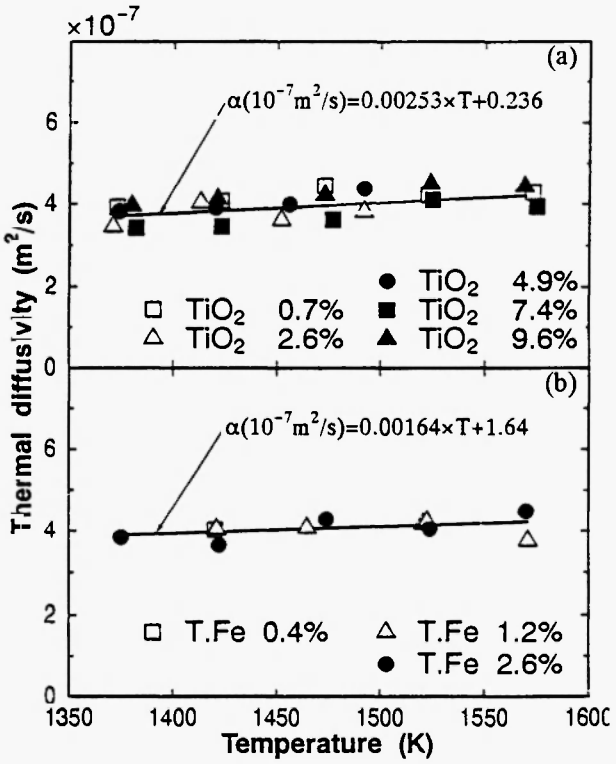

Fig. 8: Thermal diffusivity values of samples containing TiO_2 and iron oxide. These values precisely exclude the contribution due to radiative component at high temperature.

4. CONCLUDING REMARKS

Thermal diffusivity measurements of continuous casting powders for steel with various compositions have systematically been made at high temperature by the three layered laser flash method. A reference sample consists of 35.6% SiO_2, 19.9 CaO, 17.1% CaF_2, 7.7% 10.1% Na_2O, 9.3% MgO and Al_2O_3 (in mass %) and a certain amount of TiO_2, ZrO_2, HfO_2 or iron oxide is added. The thermal diffusivity values were estimated with sufficient reliability by separating the radiative component from measured values after due consideration for the variation of the absorption coefficients of respective samples. The thermal diffusivity values of continuous casting powders for

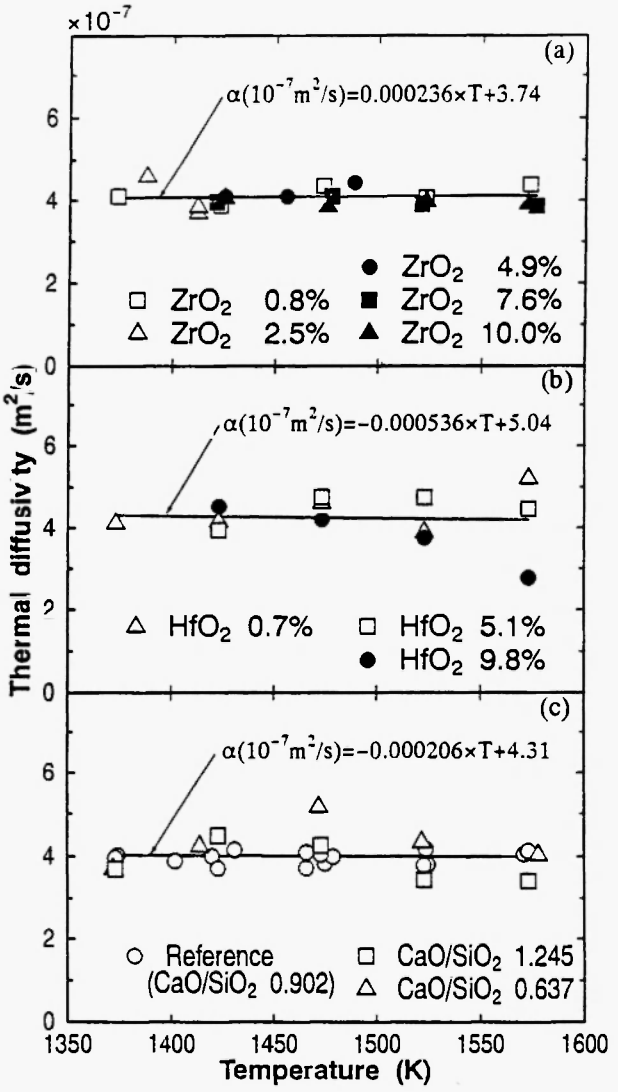

Fig. 9: Thermal diffusivity values of samples containing ZrO_2 and HfO_2 or with different CaO/SiO_2 ratio. These values precisely exclude the contribution due to radiative component at high temperature.

steel are found to be 4 ± 0.5 x 10^{-7} m^2/s and relatively insensitive to the variation of temperature and concentration presently investigated.

REFERENCES

1. K.C. Mills, *Proc. 4th Inter. Conf. on Molten Slags and Fluxes*, Iron Steel Institute of Japan (1992), p. 405.
2. H. Ohta, G. Ogura, Y. Waseda and M. Suzuki, *Rev. Sci. Intrum.*, **61**, 2645 (1990).
3. Y. Waseda, M. Masuda and H. Ohta, *Proc. 4th Inter. Symp. on Advanced Nuclear Energy Research*, Japan. Atomic Energy Research Institute (1992), p. 298.
4. H.M. James, *J. Appl. Phys.*, **51**, 4666 (1980).
5. Y. Waseda, H. Ohta, K. Watanabe, H. Shibata and K. Nakajima, *J. High temp. Soc. Japan*, **20**(3), 104 (1994).
6. H. Ohta, K. Watanabe, K. Nakajima and Y. Waseda, *High Temp. Mater. & Process.*, **12**, 139 (1993).
7. H. Ohta, K. Nakajima, M. Masuda and Y. Waseda, *Proc. 4th Inter. Symp. on Slags and Fluxes*, Iron Steel Inst. Japan, Tokyo (1992), p. 421.
8. M.I. Darby, *High Temp. High Pressure*, **15**, 629 (1983).
9. E.R. Eckert and R.M. Drake Jr., *Analysis of Heat Transfer*, McGraw-Hill Kougakusha, Tokyo (1972), p. 254.
10. S. Rosseland, *Theoretical Astrophysics*, Clarendon Press, Oxford (1936); cited in a book of R. Siegel and J.R. Howel, *Thermal Radiation Heat Transfer*, McGraw-Hill Kougakusha, Tokyo (1972), p. 470.
11. H. Ohta, M. Masuda, K. Watanabe, K. Nakajima, H. Shibata and Y. Waseda, *J. Iron & Steel Inst. Japan*, **80**(6), 463 (1994).

APPENDIX

The theoretical temperature response of three layered cell systems has been derived considering energy transfer by radiation combined with conduction for the configuration of the infinite three layered slab.

The change of the radiation intensity I_λ incident normally on volume element of liquid of thickness dx as a result of absorption is

$$dI_\lambda = -\kappa_\lambda I_\lambda dx. \qquad \text{(A1)}$$

The λ is the wave length. The κ_λ is the absorption coefficient of the liquid layer.

The radiation energy emitted from the volume

element dV is

$$dq_\lambda = 4n^2\kappa_\lambda e_{b,\lambda}dV. \quad \text{(A2)}$$

The n is the refractive index of the liquid. The $e_{b,\lambda}$ is spectral emissive power of blackbody and denoted as follows:

$$e_{b,\lambda} = \frac{2\pi c^2 h}{\lambda^5}\frac{1}{\exp(ch/\lambda kT) - 1} \quad \text{(A3)}$$

where c,h,k,T are speed of light in vacuum, Planck's constant, Boltzmann constant and absolute temperature, respectively.

The radiation energy emitted from surface dA of emissivity ε to the medium of refractive index n to the direction ψ in the $d\omega$ is

$$dq_\lambda = \varepsilon\frac{e_{b,\lambda}}{\pi}\cos\psi\, d\omega\, dA. \quad \text{(A4)}$$

The ψ is measured from the direction normal to the surface. The $d\omega$ is the solid angle.

The energy balance equation for control volume method is

$$Q_i = -k_c\frac{\theta_i - \theta_{i-1}}{x_i - x_{i-1}}\Delta t + F(x_i)\Delta t \quad \text{(A5)}$$

where x_i, θ_i, k_c and $F(x_i)$ is representative temperature in volume V_i, absolute temperature, thermal conductivity and the net radiative energy flows into unit volume par unit time, respectively. The temperature after Δt is derived from the heat capacity of V_i and Q_i.

For transparent liquid phase, considering heat equilibrium before laser pulse heating and Taylor expansion, F is

$$F = \frac{\varepsilon}{2-\varepsilon}\cdot 4n^2\sigma T_0^3[\theta(0) - \theta(l_2)]. \quad \text{(A6)}$$

T_0 is equilibrium temperature before laser pulse heating. The $\theta(0)$ and $\theta(l_2)$ are the temperature rises of upper and lower metallic layer from T_0, respectively. The F is denoted as $F = 4\varepsilon\sigma T_0^3\theta$ on outer surface of platinum plate to vacuum.

For the gray body approximation, F in liquid phase is

$$\begin{aligned}F(x) = {} & 2\Big\{\Delta e_b(0)[R_1(x) - R_4(2l_2 - x)] \\ & + \Delta e_b(l_2)[R_{1x}(l_2 + x) - R_{4x}(l_2 - x)]\Big\} \\ & + 2\kappa\int_0^{l_2}\Delta e_b(x')[R_2(2l_2 + x - x') + R_{30}(x + x') \\ & - R_{2L}(2l_2 - x + x') - R_{3L}(2l_2 - x - x')]dx' \\ & + 2\kappa\int_0^{x}\Delta e_b(x')E_2(x - x')dx' \\ & - 2\kappa\int_x^{l_2}\Delta e_b(x')E_2(x' - x)dx' \end{aligned} \quad \text{(A7)}$$

Where

$$E_2(y) = \int_0^1 \exp(-\kappa y/\mu)d\mu \quad \text{(A8)}$$

$$R_1(y) = \int_0^1 \frac{\varepsilon\mu}{\beta(\mu)}\exp(-\kappa y/\mu)d\mu \quad \text{(A9)}$$

$$R_{1x}(y) = \int_0^1 \frac{\mu}{\beta(\mu)}(1-\varepsilon)\varepsilon\exp(-\kappa y/\mu)d\mu \quad \text{(A10)}$$

$$R_2(y) = \int_0^1 \frac{1}{\beta(\mu)}(1-\varepsilon)^2\exp(-\kappa y/\mu)d\mu \quad \text{(A11)}$$

$$R_{2L}(y) = \int_0^1 \frac{1}{\beta(\mu)}(1-\varepsilon)^2\exp(-\kappa y/\mu)d\mu \quad \text{(A12)}$$

$$R_{30}(y) = \int_0^1 \frac{1}{\beta(\mu)}(1-\varepsilon)\exp(-\kappa y/\mu)d\mu \quad \text{(A13)}$$

$$R_{3L}(y) = \int_0^1 \frac{1}{\beta(\mu)}(1-\varepsilon)\exp(-\kappa y/\mu)d\mu \quad \text{(A14)}$$

$$R_4(y) = \int_0^1 \frac{\varepsilon'}{\beta(\mu)}(1-\varepsilon)\exp(-\kappa y/\mu)d\mu \quad \text{(A15)}$$

$$R_{4x}(y) = \int_0^1 \frac{\varepsilon\mu}{\beta(\mu)}\exp(-\kappa y/\mu)d\mu \quad \text{(A16)}$$

$$\beta(\mu) = 1 - (1-\varepsilon)^2\exp\left(\frac{2\kappa l_2}{\mu}\right) \quad \text{(A17)}$$

$\Delta e_b(x) = 4\sigma n^2 T^3\theta(x)$, and $\theta(x)$ is temperature rise from T at x.

For the band approximation, the measured absorption spectrum of sample liquid was divided into n regions. The wave lengths of boundaries of the regions are denoted as λ_0, λ_1, ... and λ_n from short wave length to long length. F is

$$F(x) = \sum_{m=1}^{n} F_m(x). \quad \text{(A18)}$$

Where

$$
\begin{aligned}
F_m(x) \;=\; & 2\Big\{\Delta E_m(0)[R_1(x) - R_4(2l_2 - x)] \\
& + \Delta E_m(l_2)[R_{1x}(l_2 + x) - R_{4x}(l_2 - x)]\Big\} \\
& + 2\kappa_m \int_0^{l_2} \Delta E_m(x')[R_2(2l_2 + x - x') \\
& + R_{30}(x + x') \\
& - R_{2L}(2l_2 - x + x') - R_{3L}(2l_2 - x - x')]dx' \\
& + 2\kappa_m\Big\{\int_0^{x} \Delta E_m(x')E_2(x - x')dx' \\
& - \int_x^{l_2} \Delta E(x')_m E_2(x' - x)dx'\Big\}, \qquad \text{(A19)}
\end{aligned}
$$

and

$$
\Delta E_m(x) = \int_{\lambda_{m-1}}^{\lambda_m} n^2 \frac{\partial e_{\lambda b}}{\partial T} d\lambda. \qquad \text{(A20)}
$$

The κ_m corresponds to the Rosseland mean absorption coefficient for the wave length between λ_{m-1} and λ_m.